Water Leakoff During Gel Placement in Fractures: Extension to Oil-Saturated Porous Media

Bergit Brattekås[1], The National IOR Centre of Norway and University of Stavanger;
Randy Seright, New Mexico Tech; and **Geir Ersland,** University of Bergen

Summary

Crosslinked polymers extrude through fractures during placement of many conformance-improvement treatments, as well as during hydraulic fracturing. Dehydration of polymer gel during extrusion through fractures has often been observed and was extensively investigated during recent decades. Injection of highly viscous gel increases the pressure in a fracture, which promotes gel dehydration by fluid leakoff into the adjacent matrix. The present comprehension of gel behavior dictates that the rate of fluid leakoff will be controlled by the gel and fracture properties and, to a lesser extent, be affected by the properties of an adjacent porous medium. However, several experimental results, presented in this work, indicate that fluid leakoff deviates from expected behavior when oil is present in the fracture-adjacent matrix. We investigated fluid leakoff from chromium (Cr)(III)-acetate hydrolyzed polyacrylamide (HPAM) gels during extrusion through oil-saturated, fractured core plugs. The matrix properties were varied to evaluate the effect of pore size, permeability, and heterogeneity on gel dehydration and leakoff rate. A deviating leakoff behavior during gel propagation through fractured, oil-saturated core plugs was observed, associated with the formation of a capillary driven displacement front in the matrix. Magnetic resonance imaging (MRI) was used to monitor water leakoff in a fractured, oil-saturated, carbonate core plug and verified the position and existence of a stable displacement front. The use of MRI also identified the presence of wormholes in the gel, during and after gel placement, which supports gel behavior similar to the previously proposed Seright filter-cake model. An explanation is offered for when the matrix affects gel dehydration and is supported by imaging. Our results show that the properties of a reservoir rock might affect gel dehydration, which, in turn, strongly affects the depth of gel penetration into a fracture network and the gel strength during chase floods.

Introduction

The oil industry has investigated polymer gel treatments for decades because of their usefulness in both enhanced oil recovery (EOR) and hydraulic fracturing. In EOR processes, the presence of highly viscous polymer gel in the fracture network reduced the conductivity of fractures and provided improved pressure drops and increased sweep efficiency within the rock matrix during chase floods (Hild and Wackowski 1999; Kantzas et al. 1999; Sydansk and Southwell 2000; Seright et al. 2003; Portwood 2005; Willhite and Pancake 2008). In hydraulic fracturing, polymer gel is used as a fracturing fluid to open fractures and transport propping agents along the fracture length (Dantas et al. 2005).

Note that the term "polymer gel," as used in this work, refers to formed (crosslinked) polymer gel. Polymer gel is frequently injected from the surface as a gelant (a solution containing all the components of a polymer gel that has not yet crosslinked to form a highly viscous gel). Gelants have properties similar to polymer solutions and can readily flow through rock matrix (Seright et al. 2003). Gel forms when gelant is subjected to an appropriate temperature for a certain time span (gelation time), and the solution properties change significantly; Liu and Seright (2001) reported viscosities in the range of 2×10^6 cp for a common crosslinked polymer gel system, and the gel is inhibited from passing through most pore throats because of its structure (Seright 2001). Thus, crosslinked gels propagate through open fractures during injection without entering significantly into the rock matrix. Although gelant is injected, partially or fully formed polymer gel may enter the fractured formation from the wellbore, or gel may form shortly after injection, depending on properties such as reservoir temperature and pumping time. This paper discusses the propagation of fully formed polymer gel through fractures in hydrocarbon reservoirs and assumes that formed gel propagates through fractures during most of the placement process. Many commonly used polymer gels [e.g., the Cr(III)-acetate-HPAM gel used in this work] lose water (dehydrate) during extrusion through fractures. Gel dehydration, also termed leakoff, was observed and quantified during gel propagation through fractures in several previous publications (e.g., Seright 1995, 1999, 2001, 2003a, b; Brattekås et al. 2015). Water leakoff from gel controlled the rate of gel propagation into a reservoir (Seright 2003a), as well as the rate of fracture growth during hydraulic fracturing (Howard and Fast 1957, 1970; Penny and Conway 1989). When leakoff occurs during gel injection, a higher volume of gel is required to reach a given distance in the reservoir than anticipated from the fracture volume. A high degree of leakoff reduces the efficiency of hydraulic fracturing (Howard and Fast 1957), and may also significantly affect post-treatment gas production (Barati et al. 2009). Leakoff also increases the gel concentration and resistance to washout (Brattekås et al. 2015), which can improve the gel fracture-blocking ability during subsequent EOR injections. Regardless of the purpose of the polymer gel treatment, an accurate understanding and description of leakoff in fracture systems is necessary.

Water leakoff has been described by two models: the Carter model (Howard and Fast 1957, 1970; Penny and Conway 1989) and the alternative Seright model (Seright 2003a), which represent the present understanding of gel behavior during injection. The models propose that the rate of water leakoff is controlled by gel and fracture properties and, to a lesser extent, are affected by the properties of an adjacent porous medium. The Carter and Seright models are similar on a macroscopic scale (i.e., the rate of water leakoff linearly decreases when plotted vs. time on a log-log plot) **(Fig. 1).** The leakoff rate will be further discussed in the present work. The two models are, however, fundamentally different in terms of gel behavior during placement. In particular, the models describe the formation of a concentrated gel filter cake in the fracture differently (Fig. 1). An important assumption in the Carter model is that the filter

[1] now at the Department of Physics and Technology, University of Bergen

This paper (SPE 190256) was accepted for presentation at the SPE Improved Oil Recovery Conference, Tulsa, 14–18 April 2018, and revised for publication. Original manuscript received for review 22 January 2018. Revised manuscript received for review 6 September 2018. Paper peer approved 14 November 2018.

cake forms uniformly on the fracture surface during water leakoff (i.e., the thickness of the filter cake on the fracture faces was uniform at any given time). Seright proposed the formation of an areally and volumetrically heterogeneous filter cake that forms when fragments of injected gel dehydrated and settled in the vicinity in which the dehydration occurred (i.e., the filter cake was nonuniformly distributed in the fracture volume). Recent advances in in-situ imaging supported the existence of a randomly distributed filter cake in the fracture volume (Brattekås et al. 2016).

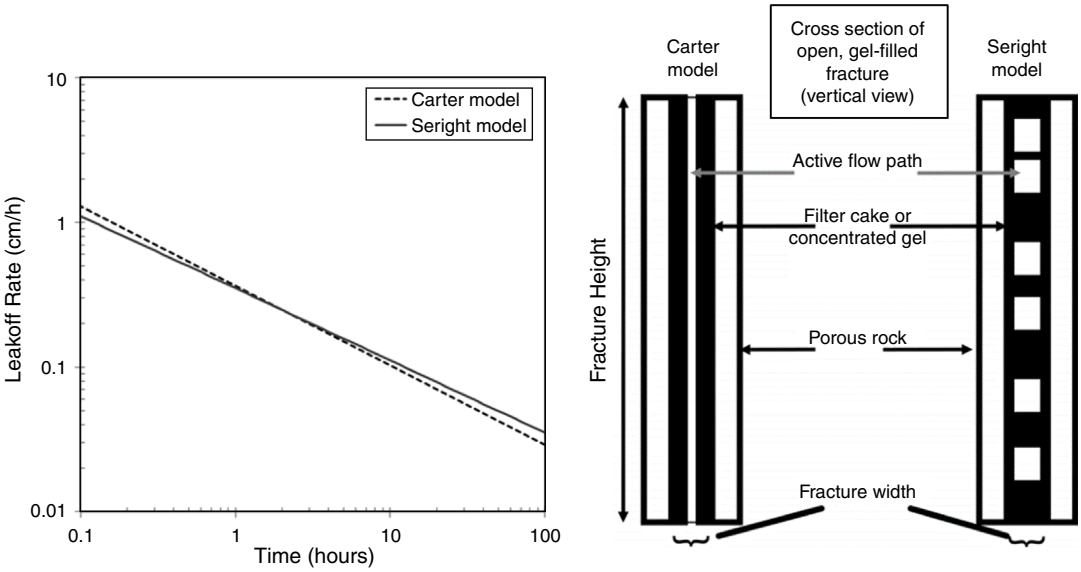

Fig. 1—Two common models used to predict fluid leakoff from polymer gel: the leakoff model by Carter and the alternative leakoff model by Seright. Left: The macroscopic behavior of gel (i.e., leakoff rates vs. time) is similar in both models. Right: Filter-cake formation differs significantly between the two models (figure modified from Seright 2003a).

The leakoff rates predicted by the Seright model are based on experimental work, in which gel was injected into longitudinal fractures through porous rock core plugs. The core plugs were saturated by water corresponding with the water bound in gel (the gel solvent). In rocks saturated by water only, saturation functions (capillary pressure and relative permeability) are not present in the matrix and, consequently, do not influence gel placement.

Saturation functions are, however, important when considering fractured hydrocarbon reservoirs, in which oil is also present in the rock matrix. We investigated water leakoff from Cr(III)-acetate-HPAM gels during extrusion through oil-saturated, fractured core plugs. The work presented in this paper was motivated by an attempt to understand when (and if) the properties of the rock matrix influence water leakoff, and why and when the measured leakoff properties deviate from expected behavior.

Experiments

Core Preparations. Cylindrical core plugs were drilled from large outcrop rock blocks of different core materials:

- Rørdal chalk from Aalborg in Denmark (Ekdale and Bromley 1993; Hjuler and Fabricius 2007), in which the porosity and absolute permeability values for core plugs used in this work ranged from $\phi = 43$ to 46% and $k = 3$ to 10 md, respectively. Rørdal chalk has small pore throats and is expected to be homogeneous.
- Edwards Limestone from west Texas, USA (Tie 2006; Johannesen 2008), in which trimodal pore sizes, vugs, and microporosity have been identified. A variation in porosity and absolute permeability values, ranging from $\phi = 16$ to 24% and $k = 3$ to 28 md, was found to be representative of the large rock block from which cores were drilled for this work.
- Bentheimer sandstone from Bentheim, Germany (Schutjens et al. 1995; Klein and Reuschle 2003), is a homogeneous sandstone with large pore throats and porosity and absolute permeability values averaging $\phi = 23\%$ and $k = 1{,}100$ md.

The cores were cut to length (5 to 9 cm), and a band saw was used to create smooth, longitudinal fractures through each core plug. The cores were assembled with open fractures; polyoxymethylene (POM) spacers were placed along the top and bottom of the fracture to maintain a constant fracture aperture of 1 mm. Some cores were assembled with different rock materials on each side of the fracture (e.g., a Rørdal chalk core half was assembled with a Bentheimer sandstone core half or an Edwards Limestone core half to create a contrast in properties on each side of the fracture). The core circumference and outlet end faces were covered in several layers of epoxy to prevent flow and to enable the cores to withstand elevated pressures. The inlet end faces were left open to flow. POM end pieces were glued to the inlet and outlet end face to connect the cores to injection and production lines. Holes were drilled through the epoxy 1 cm from the outlet end face of each core half. Short pieces of 1/8-in. stainless-steel tubing were positioned into the holes and glued in place, to be used as matrix production outlets. Core 8RC was placed in an MRI for imaging of gel placement, thus stainless-steel tubing pieces were omitted. Core 8RC features a specially designed POM end piece at the outlet end face, facilitating three production outlets, one for the fracture and one for each core half. The core plug properties are found in **Table 1.**

The core preparation procedure required the core material to be dry during assembly (for two reasons: 1) the epoxy glue did not stick well to wet surfaces, and 2) the procedure took several hours/days to complete, at which time saturated core plugs were prone to significant evaporation and associated uncertainties). The length (L), fracture height (H), and maximum thickness (r_{max}) were measured for each core half before assembly. All cores were saturated directly with mineral oil (n-decane) under vacuum after finalized assembly. This ensures fully oil-saturated cores at the start of gel injection. Air production or other contradictions to the assumption of fully oil-saturated cores were not observed during the experimental work. The n-decane was filtered through glass wool and silica gel before use, to remove polar components, and should not influence core wettability, which is assumed to be strongly water-wet in this study. Average porosities and pore volumes (PVs) were determined from weight measurements. In cores where the core halves were of

different core materials, porosities and PVs were estimated using a simple matching procedure; the total PV for the system, provided from weight measurements, was corrected for fracture and tubing volumes. The porosities of Core Half 1 (CH1) and Core Half 2 (CH2) were adjusted within the ranges specified previously, until the sum of the calculated PVs corresponded to the total PV. The permeability contrast for each system (K_{ratio}) was approximated using assumed absolute permeability values of 6 and 1,100 md for chalk and sandstone, respectively, while Edwards Limestone permeabilities were estimated from porosity using a linear approximation (Haugen et al. 2008).

Core Identification	K_{ratio}	Core Half	Core Material	L (cm)	H (cm)	r_{max} (cm)	Porosity (%)	PV (mL)
1EDW	1	CH1	Edwards Limestone	7.18	4.78	2.12	25.5	12.9
		CH2	Edwards Limestone	7.18	4.78	2.28	25.5	15.1
2BS	1	CH1	Bentheimer sandstone	6.94	4.91	2.24	23.0	15.0
		CH2	Bentheimer sandstone	6.94	4.92	2.41	23.0	15.2
3RC	1	CH1	Rørdal chalk	8.63	3.79	1.76	46.0	19.3
		CH2	Rørdal chalk	8.61	3.79	1.84	46.0	21.1
4BS_EDW	39	CH1	Bentheimer sandstone	7.30	5.16	2.54	30.0	22.3
		CH2	Edwards Limestone	7.19	4.88	2.34	27.0	16.8
5BS_EDW	86	CH1	Bentheimer sandstone	7.40	5.14	2.54	30.0	21.9
		CH2	Edwards Limestone	7.27	4.91	2.53	21.0	15.5
6EDW_RC	10	CH1	Rørdal chalk	5.95	5.08	2.43	46.0	25.8
		CH2	Edwards Limestone	5.90	4.88	2.36	40.0	19.7
7BS_RC	183	CH1	Rørdal chalk	6.04	5.07	2.52	45.0	27.4
		CH2	Bentheimer sandstone	5.57	5.11	2.53	23.0	13.3
8RC	1	CH1	Rørdal chalk	7.61	4.92	2.34	46.6	35.6
		CH2	Rørdal chalk	7.61	4.91	2.34	46.6	35.6

Table 1—Core properties.

Gel Injection. Five thousand ppm of HPAM polymer (5 million Daltons molecular weight, degree of hydrolysis 10 to 15%) was mixed in brine [4 wt% sodium chloride (NaCl), 3.4 wt% calcium chloride ($CaCl_2$), 0.5 wt% magnesium chloride ($MgCl_2$), 0.05 wt% sodium nitrate ($NaNO_3$)] until completely dissolved, and 417 ppm Cr(III)-acetate crosslinker was added to the solution to make gelant. The gelant was placed in an accumulator at an elevated temperature of 41°C for 24 hours (approximately five times the gelation time) to form gel. The crosslinked polymer gel was cooled to ambient conditions (≈23°C) before injection into the open fractures. The gel used for Core 8RC was based on a deuterium (D_2O) brine but followed the same procedure. Brattekås et al. (2015) injected Cr(III)-acetate-HPAM gel into water-saturated core plugs of the same chalk and sandstone core material as used in the present work. Gel-injection rates of 200 mL/h and higher yielded leakoff rates that followed the Seright model (i.e., the gel behaved as predicted during injection). Therefore, a gel-injection rate of 200 mL/h was chosen for the present experiments, in which the core plugs were fully oil-saturated at the start of gel injection. Gel injection continued for approximately 4 hours (≈800 mL of gel). The fracture volume (FV) ranged from 3 to 4 mL; hence, more than 200 FV of formed gel was extruded through the core plugs in these experiments. The injection pressure at the fracture inlet and effluents from each core half, produced through the matrix production outlets, were measured with time during gel injection. The experimental setup is shown in **Fig. 2.** Core 8RC was placed in an MRI for imaging during gel injection and the experimental setup (shown in **Fig. 3**) therefore differed slightly from that of the other experiments.

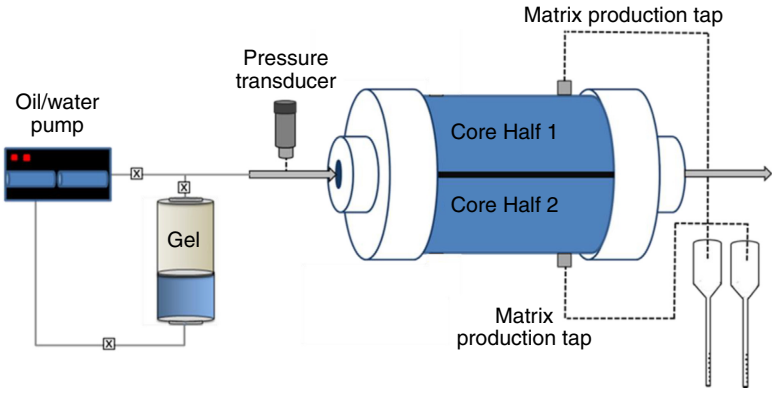

Fig. 2—Schematic of experimental setup for gel injection into fractured cores. The fluids produced from each core half were logged separately vs. time.

Results and Discussion

Gel Injection Into Fractured, Oil-Saturated Core Plugs. The water-leakoff rate during gel injection is commonly calculated on the basis of measurements of the produced effluent volume through a rock matrix (in this paper and in Brattekås et al. 2015, 2016b; Seright

1995, 1999, 2001, 2003a,b); the effluent volumes were recorded vs. time (both oil and water were produced through the matrix in this work), and divided by the fracture surface area and time interval between measurements to calculate the leakoff rate. Because different core materials were used on each side of the fracture in many of the experiments (Table 1), the produced fluids were measured separately for each core half in this work. On the basis of the volume of oil produced from each core half vs. time, we expected to be able to calculate the saturation development in each core half. In cores with a permeability contrast between the core halves, however, this was not straightforward. Because of gel dehydration, several FVs of gel must be injected before gel breakthrough is observed at the producing end (termed "outlet") of the core. During this time, we observed (1) production of more than 1 FV of oil from the fracture production outlet. Some of this oil originates from the matrix but cannot be assigned to a specific core half in opaque systems. Or, we observed (2) no oil production from the fracture outlet, but significant oil production from the more permeable core half (total volume of oil produced through one matrix production outlet frequently exceeding the PV of the core half). These artifacts, associated with the use of small core plugs with a strong water-wetting preference, made direct calculations of saturation challenging; thus, normalized water-saturation developments are given in the figures in this section (saturations were normalized to the total volume of oil produced from the respective matrix production outlet).

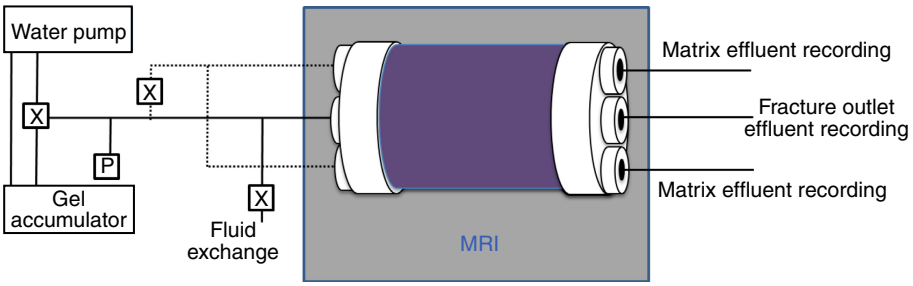

Fig. 3—Experimental setup for Core 8RC, placed in an MRI during injection of D_2O-based polymer gel.

Sandstone. Formed polymer gel was injected into oil-saturated Bentheimer sandstone cores. Because of large pore throats, associated high permeability and low capillarity were expected for this core material. **Fig. 4** shows leakoff rates calculated from effluent recordings during gel injection into 2BS (both core halves were sandstone) and composite cores; sandstone core halves assembled with another core material on the opposite side of the fracture (chalk in Core 7BS_RC, limestone in Cores 4BS_EDW and 5BS_EDW).

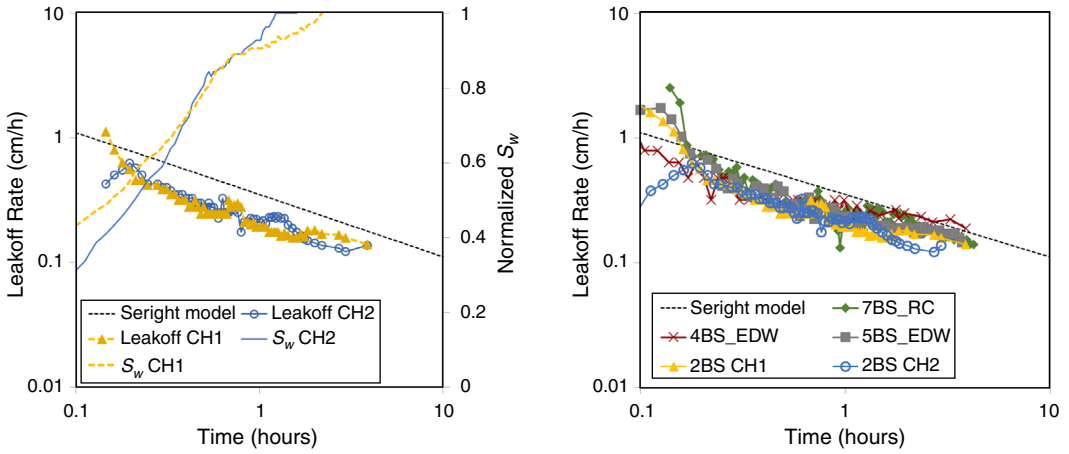

Fig. 4—Effluents produced from sandstone core halves during gel injection formed the basis for leakoff-rate calculations. Left: Water-leakoff rate in Core 2BS, where both core halves were of sandstone material. Right: Leakoff rates for all sandstone core halves: sandstone coupled with sandstone, limestone, and chalk. S_w = water saturation.

The measured leakoff rates decreased linearly on a log-log plot, with values lower than predicted by the Seright leakoff model, but with a similar slope. The type of core material on the opposite side of the fracture did not affect the leakoff rates through the sandstone core halves, although the volume of oil produced through the sandstone varied and was higher when sandstone was assembled with chalk. The small reduction in leakoff rate compared with the Seright model will be discussed in the section Gel Dehydration on the Core Scale.

Limestone. A trimodal pore-size distribution, with both microporosity and vugs, was identified in previous studies of the Edwards Limestone core material (Johannesen 2008), thus significant local variations in permeability and capillarity are expected. Effluents produced from each matrix production outlet during gel injection formed the basis for leakoff calculations. Leakoff rates for limestone core halves are shown in **Fig. 5** and deviated from the expected results (i.e., the Seright model). During early-stage gel injection, oil was produced from the matrix production outlets, and the leakoff rates decreased similar to the Seright model, exhibiting a nearly linear trend on a logarithmic rate/time plot. At the start of two-phase production (oil and water) from the matrix production outlets, a swift decrease in leakoff rate was observed. After the production of oil ceased, only water was produced from the matrix outlets, and a nearly constant leakoff rate was measured for the remaining gel injection. This trend was similar for all limestone core halves, both when the same core material was used on each side of the fracture (Core 1EDW in Fig. 5) and when limestone was assembled with sandstone (4BS_EDW and 5BS_EDW) or chalk (6EDW_RC) on the opposite side of the fracture. The leakoff-rate plateau (nearly constant leakoff rate observed when water was produced alone through the matrix outlets) varied between core halves regardless of the core material with which limestone was assembled. This might be explained by the inherent heterogeneity of the limestone core material.

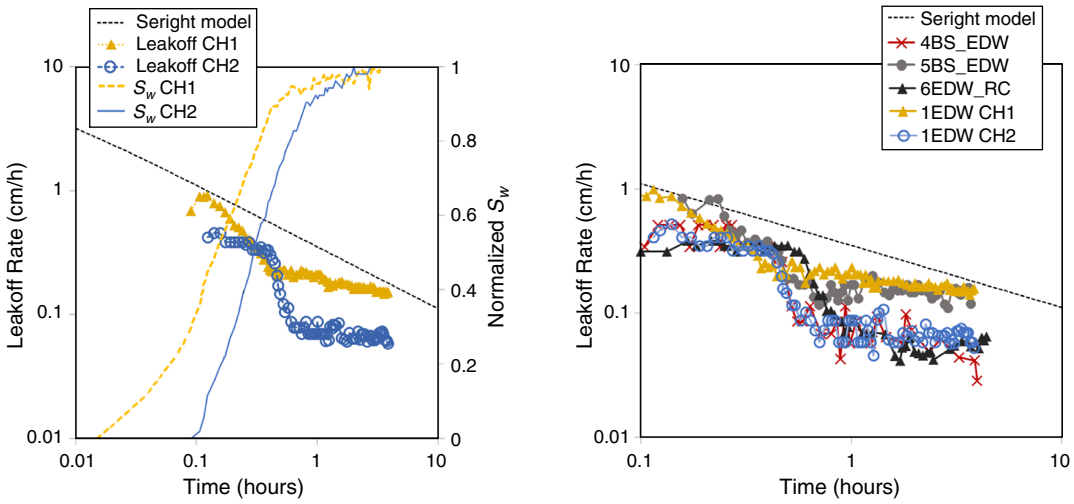

Fig. 5—Effluents produced from limestone core halves during gel injection formed the basis for leakoff-rate calculations. Left: Leakoff rate for Core 1EDW (both core halves limestone). Right: Leakoff rates for all limestone core halves: limestone coupled with limestone, sandstone, and chalk. S_w = water saturation.

Chalk. Rørdal chalk is usually considered to be homogeneous, without significant variations in pore size. **Fig. 6** shows the leakoff rates for chalk, calculated from produced effluents from chalk production outlets during gel injection. During early-stage gel injection, oil alone was produced from the matrix taps, and the leakoff rates followed a decreasing trend similar to that predicted by the Seright model. At $t \approx 0.8$ hours of gel injection, the leakoff rates swiftly decreased, corresponding with the start of two-phase (oil and water) production from the matrix production outlets. From $t = 1.2$ hours, only water was produced out of the matrix taps, and the leakoff rates were nearly constant and lower than expected. Core 3RC was assembled with chalk on both sides of the fracture. The leakoff rates and saturation developments were equal on both sides of the fracture (i.e., the behavior in each core half replicated the other). This could be expected because of the homogeneity of the chalk core material. When chalk was assembled with sandstone (7BS_RC) or limestone (6EDW_RC) on the opposite side of the fracture, the chalk leakoff rates appeared to be influenced by the core material on the other side of the fracture. This is consistent with the observation of oil mainly being produced through the more permeable core half, as previously discussed.

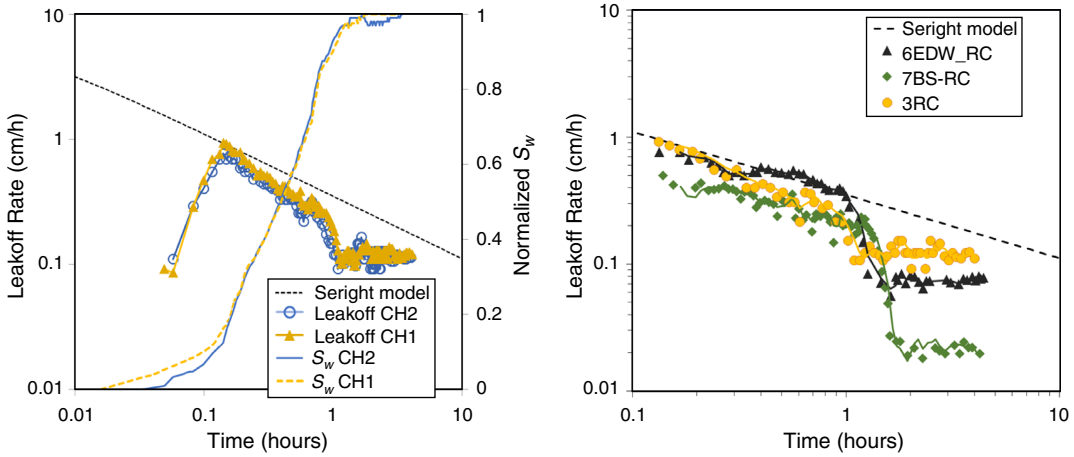

Fig. 6—Effluents produced from chalk core halves during gel injection formed the basis for leakoff-rate calculations. Left: Leakoff in Core 3RC (both core halves chalk). Right: Leakoff rates for all chalk core halves: chalk coupled with chalk, limestone, and sandstone. S_w = water saturation.

Fully water-saturated cores within a range of different permeabilities and pore-size distributions were previously used to investigate gel dehydration (see Seright 2003a), without influencing the measured leakoff rates. In this work, the presence of oil in the rock matrix was observed to influence water leakoff (Figs. 4 through 6), where leakoff rates varied with core material and oil saturation. Saturation functions (relative permeability and capillary pressure) are not present in fully water-saturated rocks but dictate fluid flow in two-phase saturated porous media. Rock properties (e.g., permeability and pore size) strongly influence saturation functions, which may, in turn, influence gel dehydration.

Understanding the observed leakoff behavior and interpreting it in terms of saturation and saturation functions was not straightforward. Imaging by MRI was applied to gain insight into in-situ fluid flow during gel extrusion through fractures. In chalk, small variations in pore size within the core material were expected (i.e., the capillary pressure varies less with location). A pronounced and reproducible effect on the leakoff behavior was also observed in chalk during initial experiments (Fig. 6). Therefore, MRI was performed on Rørdal chalk Core 8RC during gel injection, seeking to understand the apparent effect of oil saturation and core material on leakoff rate.

Visualization of Leakoff Using MRI. The leakoff rates presented in Figs. 4 through 6 were based on volumetric measurements of produced effluents from the matrix during gel injection; the leakoff rate was then calculated by dividing the produced volume by the fracture surface area, and the time increment between measurements. The resulting leakoff rate is given as (distance/time) and can theoretically be related to the velocity of leakoff water passing through a rock matrix. Using MRI, the position of water flowing away from a fracture surface and into an oil-saturated rock matrix can be accurately determined and leakoff water velocity calculated.

Oil-saturated chalk Core 8RC was placed in a 4.7-Tesla Biospec MRI to investigate water leakoff during D_2O-gel extrusion through an open fracture. Gel dehydration caused D_2O brine to leave the gel and invade the rock matrix. The magnetic signal from oil initially in place was removed when the oil was displaced by D_2O. The displacement front was detected by the MRI as the interface between hydrocarbon (signal) and D_2O brine (no signal) and was recorded with time. 2D image slices in the coronal direction (Brattekås and Fernø 2016) were acquired during D_2O-gel injection in the MRI to limit acquisition time and accurately capture the water-leakoff process. The acquisition time for a coronal slice was 1 minute 42 seconds. **Fig. 7** shows snapshots of gel injection into Core 8RC. The top left corner of the figure shows the initial state of the core before gel injection started. The bright white line is bulk oil initially saturating the fracture. The light gray areas are rock matrix saturated by oil. Most of the bulk oil signal in the fracture disappeared when gel started to extrude through the fracture (shown at approximately $t = 5$ minutes) (i.e., the oil was displaced). Some of the oil signal, however, remained visible in parts of the fracture. The signal was stable, both in terms of strength and position, throughout gel injection, hence this was not indicative of countercurrent production of oil into the fracture. Further investigations showed that the signal was attributed to oil captured within the gel structure. In experimental work where calculations rely on material balance, the entire bulk volume of oil is expected to be produced from the fracture before gel breakthrough. The departure from this assumption, observed by MRI, can influence the saturation development reported in conventional core-scale experiments.

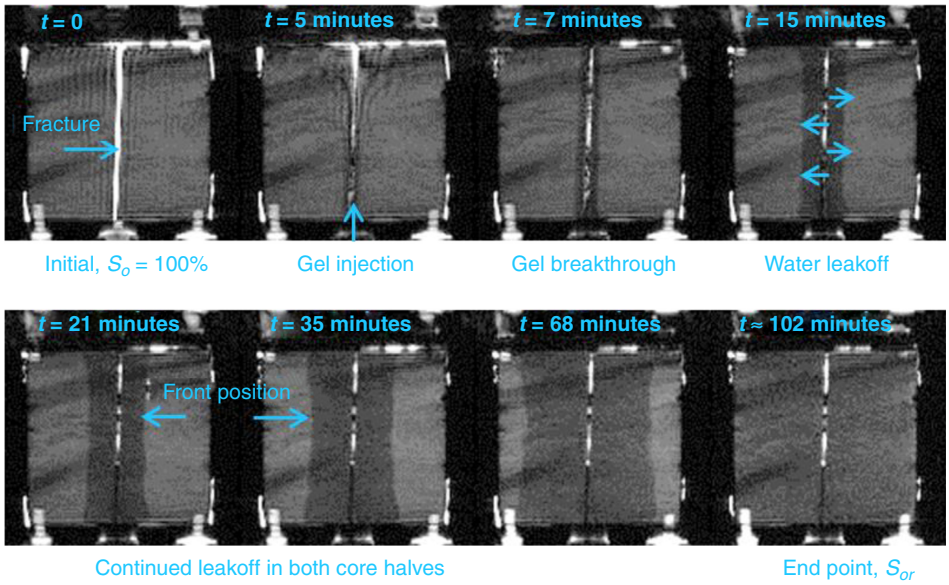

Fig. 7—Snapshots of water leakoff during gel injection into Core 8RC, obtained using MRI. The images show the gel-dehydration process in the middle of the cylindrical core (top-down). S_o = oil saturation; S_{or} = residual oil saturation.

Gel breakthrough was observed at the fracture outlet at $t \approx 7$ minutes; after that, water leakoff was clearly visible in the rock matrix. The position of the D_2O-water front was identified by MRI at all times, as demonstrated in Fig. 7. Leakoff water can be seen as the dark gray areas in the images, displacing the light gray oil signal away from the fracture surfaces. The leakoff water displaced oil uniformly outward from the fracture, which suggests that capillary forces strongly influenced the displacement process in the matrix. The flow of leakoff water within the matrix was detectable by MRI for as long as oil was dynamically displaced (i.e., during the timeline given in Fig. 7). Images acquired using MRI during the first 102 minutes of gel injection, during which leakoff could be determined by imaging, was analyzed using basic image analysis software (ImageJ[2]), to extract the front position for several timesteps. The velocity of the leakoff water front was then calculated directly by dividing the front location with time.

The velocity of the leakoff water front given by MRI is shown in **Fig. 8.** Effluent measurements were only available at designated times during gel injection because of restrictions in entering the MRI facilities during imaging; the available leakoff-rate points are included in the figure. The leakoff rate based on the effluents corresponds well with the previous experiments using chalk core material, presented in Fig. 6. However, the measured front velocity using MRI does not resemble the leakoff rate calculated from effluent measurements. Nor does it follow the path predicted by the Seright model [although it should theoretically correspond to the (distance/time) parameter given by the model], but it yields a higher rate and lower decline vs. time. Fig. 8 shows leakoff rates from one experiment, calculated to be both higher and lower than expected, using two different measuring methods. A mismatch between volumetric and directly measured leakoff rates could easily be ascribed as erroneous if reported for different experiments. Fig. 8, however, shows different leakoff rates for the same leakoff process, in which the difference must be attributed to the measuring and calculation methods and be directly related to our understanding of leakoff itself.

After gel injection, H_2O brine (composition corresponding to the D_2O brine used as solvent) was injected into Core 8RC. Unlike the D_2O brine, H_2O brine provides a signal detectable by MRI. The gel-rupture pressure was measured at 15.7 psi/ft, which corresponds well with previously measured rupture pressures at the same gel-injection rate and throughput (Brattekås et al. 2015). After gel rupture, water can pass through the gel-filled fracture. **Fig. 9** shows a 3D image of Core 8RC during waterflooding. The matrix was at residual

[2] ImageJ is an open-source, Java-based image processing program developed at the National Institutes of Health and the Laboratory for Optical and Computational Instrumentation at the University of Wisconsin.

oil saturation (S_{or}) during waterflooding, with D_2O constituting the water phase. Therefore, the majority of the signal was detected in the fracture. Two fluids were responsible for the signal—oil coating the gel (purple in Fig. 9) and H_2O brine flowing through the gel (yellow color). The H_2O brine was distinguishable from the oil phase by proper thresholding of the MRI images. Water flow through the gel-filled fracture was observed to occur in narrow flow channels, often termed wormholes. The wormholes appear randomly distributed in the fracture, which supports the Seright-model description of a randomly distributed filter cake in the fracture volume. Therefore, it is likely that gel dehydration (leakoff) occurred in a manner similar to the description by Seright (2003a), and we used the Seright model as a basis for further analysis of leakoff properties in this paper.

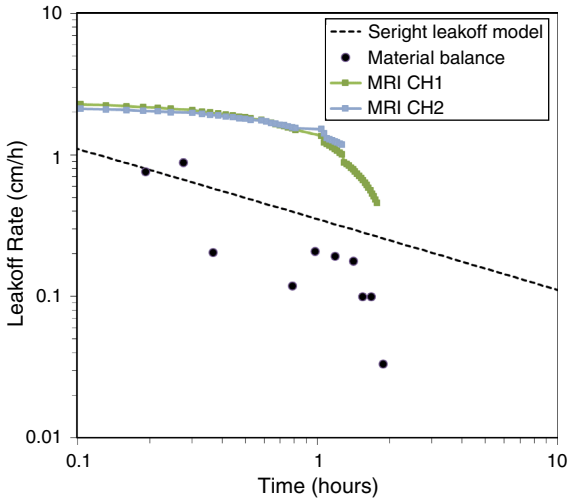

Fig. 8—Leakoff rate for an oil-saturated chalk core plug determined by direct measurements of front location/time by MRI (blue and green lines) compared with leakoff rate calculated from produced effluents (black dots) and the Seright model (black, dotted line).

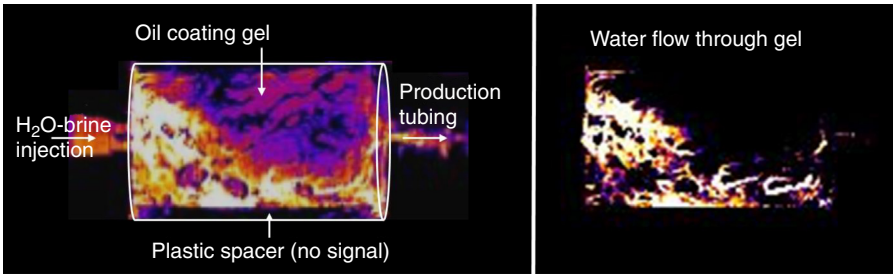

Fig. 9—H_2O-brine injection into the gel-filled fracture of Core 8RC. Left: 3D image of the core. The signal shown comes from the fracture only. The purple signal is oil coating the gel. Right: With proper thresholding, the signal from H_2O brine can be distinguished. Water moves through the gel-filled fracture through a network of narrow flow channels (wormholes).

Water Leakoff in Cylindrical Cores. The commonly used models for leakoff (Seright and Carter) present the leakoff rate as a 2D velocity parameter, although a volumetric flow rate is usually experimentally measured. The conversion of 3D volumetrically measured data (the effluents) to a 2D parameter describing velocity has been unproblematic thus far; experiments have repeatedly shown that the leakoff rate corresponds with the models (measured to be linearly decreasing on a log-log plot of leakoff rate vs. time), despite significant experimental variability. Cores of different rock materials, shapes, and dimensions have been used, and gel has been injected using a variety of injection rates and volumes. Dividing the produced-fluid volume by the fracture surface area and time increments between measurements to calculate the leakoff rate has provided reproducible results.

In this work, MRI provides insight into the flooding process within the rock matrix. Water leaking off into oil-saturated chalk formed a uniform displacement front through the core matrix. The distance from the fracture to the leakoff front was equal for all core lengths (i.e., one velocity could be assigned to the front). Therefore, volumetric measurement of effluents (3D) can be related to the velocity of the fluid front (2D) in this specific core, although only theoretically in previous work. To correctly relate the leakoff water front position measured by MRI to a fluid volume, the images must be corrected for

- Porosity: the area behind the leakoff front holds rock material in addition to fluids.
- S_{or}: the pore space was initially saturated by oil. Although some of the oil is displaced by water, residual oil resides behind the leakoff front position and occupies parts of the PV.

Fig. 10 shows a schematic of gel dehydrating in an open fracture, forcing water into the matrix to displace oil, and illustrates an additional correction necessary when using cylindrically shaped cores; the volume of oil ahead of the leakoff front will decrease as the front moves closer to the core circumference (i.e., when leakoff water flows into the rock matrix close to the fracture surface, it will displace more oil than when flowing a corresponding distance farther into the rock matrix).

The argument of a uniform leakoff front with a single velocity, validated by MRI, was used to modify the Seright model to reflect the cylindrical shape of Core 8RC. Note that the Seright and Carter leakoff models are similar on macroscopic scales (i.e., in terms of expected leakoff rate), and the modifications described here would apply to either model. The Seright model was used as a basis for analysis because of the characteristic wormholes observed during waterflooding.

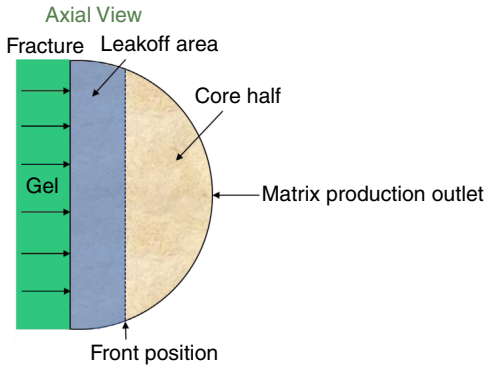

Fig. 10—Axial view of gel dehydration in an open fracture. The front position (penetration distance of leakoff water into the matrix) was measured using MRI.

Step 1: A theoretical leakoff distance was calculated for designated timesteps [the leakoff rate given by the Seright model (cm/h) was multiplied by time to provide the leakoff distance].

Step 2: Simple trigonometry was used to find the leakoff area (Fig. 10, the area behind the leakoff front) for each calculated leakoff distance.

Step 3: The leakoff area was multiplied by the fracture length for each timestep. This provides a volume that can be converted to a leakoff rate through conventional calculations (dividing the volume by fracture surface area and time increments). The converted leakoff rate provided by the Seright model and the dimensions and shape of Core 8RC are shown in **Fig. 11** (orange line).

Step 4: The modified model was corrected for estimated porosity (blue line) and S_{or} (dotted black line), respectively, to review their separate effects. To correctly reflect gel injection into an oil-saturated chalk core, the model must be corrected for both.

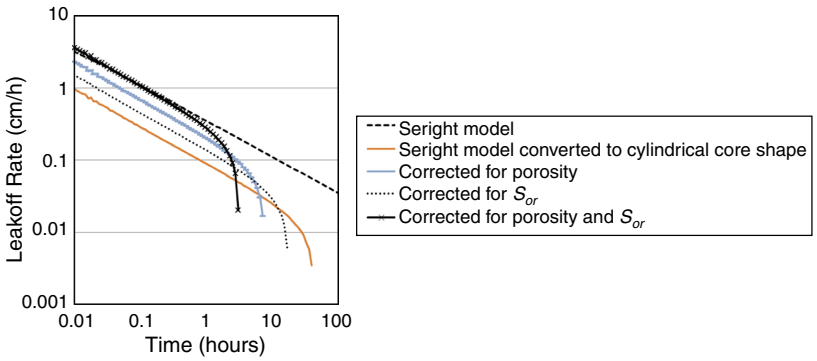

Fig. 11—Modified model for leakoff in an oil-saturated cylindrical chalk core (orange) corrected for S_{or} (black, dotted line), porosity (blue line), and S_{or} and porosity (black crosses). Note that the core diameter for these curves is fixed at 4.6 cm, corresponding to Core 8RC.

A modified Seright model, corrected for core shape, porosity, and saturation, is shown as black crosses in Fig. 11. The modified model reflects the fluid volume displaced by the front at any given timestep, and thus provides the leakoff rate expected from volumetric measurements (effluents) in cylindrical Core 8RC. Gel injection into oil-saturated chalk cores (Fig. 6) is well-captured by the modified model. A high leakoff rate, close to the original Seright model, can be expected initially. The leakoff-rate decline is faster than originally anticipated, with a sudden swift decrease. The swift decline in leakoff rate appears when the leakoff front reaches the matrix production outlets located at the core circumference. When the leakoff front approaches the core circumference, the volume of oil ahead of the front quickly diminishes, which is reflected in a smaller volume produced from the matrix. In many cylindrical cores, leakoff rates measured from effluents have corresponded well with the conventional Seright model (e.g., Brattekås et al. 2015, oil-saturated sandstone, Fig. 4). In such cases, a stable displacement front with one representative velocity cannot exist.

Fig. 12 compares the modified leakoff model to the leakoff front velocity (measured by MRI and corrected for porosity and S_{or}) and volumetric effluent measurements, respectively. Taking the core shape into account significantly improves the match between model and measurements. The swift decline in leakoff rate was observed in volumetric measurements and confirmed by MRI. This occurs when the leakoff front approaches the core circumference and is captured by the model. The transient period (two-phase production) occurs when the front reaches the production outlets and was short in chalk. The displacement front ceases to exist when the transient period is over, and leakoff water is produced through the production outlets.

The position of the leakoff front measured by MRI compared with the theoretical leakoff distance given directly by the Seright model (see Step 1) is shown in Fig. 12. The leakoff water front position measured by MRI initially reached a shorter distance into the rock than predicted by the Seright model. The declining development of the leakoff front position predicted by the Seright model, however, was not reflected in the MRI measurements, and from $t = 0.39$ hours, the leakoff front moved faster in Core 8RC and reached farther into the rock than anticipated. Note that the core shape is not accounted for in the leakoff front position given by the Seright model, which might cause these deviations.

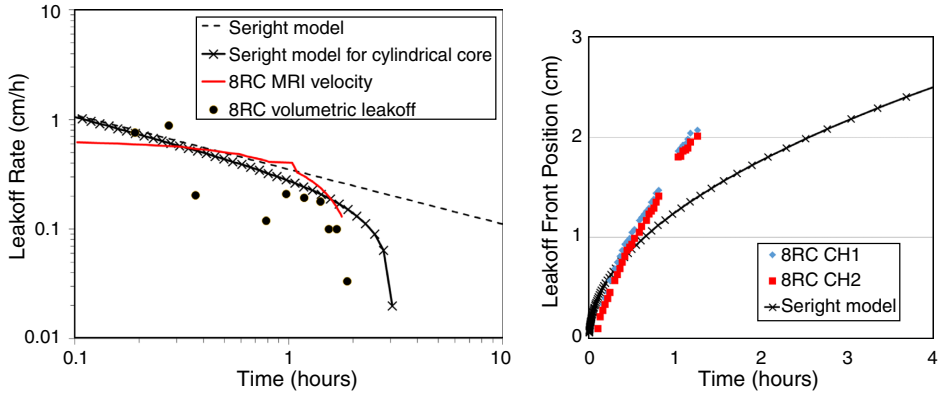

Fig. 12—Left: Leakoff rate from MRI imaging (red line), compared with the expected leakoff rate for Core 8RC on the basis of the Seright model (black crosses) and the volumetrically calculated leakoff rate (black dots). Right: The leakoff water-front position of Core 8RC measured by MRI compared with leakoff distance calculated directly from the Seright model. The front position was corrected for porosity and S_{or}.

Current Experimental Work in Context: Should the Leakoff Rate Correspond to Front Velocity? Previous leakoff experiments have repeatedly shown that gel dehydration follows the same trend, accurately described by the Seright model, in core systems of different core materials, shapes, and dimensions. In this work, we observed that the leakoff rate was determined by conditions behind and ahead of the fluid displacement front (Figs. 11 and 12), which challenge the idea of a global prediction of leakoff rate.

In experiments where the rock matrix is saturated by one phase only (often water), matrix flow is controlled by absolute permeability, given by Darcy's law. Water can flow into the matrix at any location, provided that the matrix permeability exceeds the permeability of the gel in the fracture. It is highly likely that the leakoff process is controlled by the properties of gel and where it resides (the fracture properties) in such cases, while the rock matrix acts like a filter for the gel. Our current observations propose that water leakoff is not controlled by the gel alone in all systems but is also affected by saturation functions in the rock matrix when oil is present. A uniform leakoff front outward from the fracture was observed in a chalk core by MRI. The unique velocity of the leakoff front rendered modification of the Seright model possible to accurately capture the experimental properties (e.g., core shape) and improve the match between model and experiments. Because the modifications to the leakoff model depend on the properties of the experiment, the same leakoff rate cannot be expected for varying core shapes, saturations, and, above all, wettabilities.

Leakoff was originally defined as a filtration velocity at the fracture surface, which might not be easily measured in conventional core-scale experiments. Using imaging methods to directly measure the position of the leakoff front in a porous rock should give a close approximation to the filtration velocity. Differences in porosity (also for fully water-saturated rocks) and residual saturations will influence such measurements. Further, the correlation between volumetric measurements and a filtration velocity depends on the fluids passing through a uniformly shaped media, which is not the case when using cylindrical cores. Although the notion of leakoff rate as a filtration velocity at the fracture surface is initially logical, the presentation of leakoff rate as (distance/time) on the basis of (volume/time) measured data might be dubious; water that passes from the gel through the fracture surface will not always propagate unhindered through any rock, and our measuring methods and understanding of the term "leakoff rate" will affect the results and our interpretation of the results, respectively. This was emphasized by the initial deviation between the directly (2D) and volumetrically (3D) measured leakoff rates in a cylindrical core, shown in Fig. 8. In situ imaging of gel injection into oil-saturated chalk Core 8RC showed that water displaced oil in a piston-like manner, uniformly outward from the fracture surface (i.e., the front had one representative velocity). This can be attributed to the strong capillary forces in chalk and cannot be used as a global assumption for all core systems. However; for Core 8RC, and probably for similar chalk cores, this observation connected volumetric measurements of leakoff rate to a unique leakoff distance, and the Seright model could be modified. When saturation functions are less influential on flow (e.g., sandstone) or nonexisting (water-saturated cores), matrix flow will, to a larger extent, be controlled by the pressure drop between the gel in the fracture and the matrix production outlet and is more likely to vary with fracture length. A uniform displacement front outward from the fracture is less likely to form in such systems. In these cases, we may question whether we should expect the volumetrically measured leakoff rate to correspond to a leakoff distance. We argue that the volume of water leaving the gel is more important for most applications than how far into the matrix, and how fast, the water is moving. The volume of water leaking off from the gel controls the rate of gel propagation into a reservoir, as well as the degree of gel dehydration and fracture growth during hydraulic fracturing, and is measured directly in most conventional experiments. The presentation of leakoff rate as a 2D parameter might be useful to normalize the experimental data and remove the effect of fracture volume (which is significantly different in previous experiments) on leakoff rate. The "normalized" leakoff rate is an average for the entire fracture, in which variations in gel dehydration within the fracture volume are not accounted for. Although this "normalized" leakoff rate can be used to compare leakoff experiments with the Seright and Carter models, it cannot be assumed to represent a unique velocity, or a leakoff distance, in the rock matrix in most experiments.

Gel Dehydration on the Core Scale. The current work shows that the volume of water leaving the gel (here understood as the leakoff rate) during extrusion through fractures depends on the conditions of the rock matrix (e.g., its shape and saturation). Figs. 4 through 6 indicate leakoff dependency on core material, with more pronounced deviations in high-capillarity core materials, such as chalk and limestone. A significant difference between water displacement in oil-saturated chalk and in oil-saturated sandstone is the development of a stable and capillary-driven displacement front in chalk. The forming of a stable displacement front (verified by MRI in Core 8RC) combined with the core shape explained the reproducible deviations from expected leakoff in the chalk cores, illustrated in **Fig. 13.** Relative permeability and capillary pressure curves representative of the chalk core material are also shown in the figure. Gel injection started at zero water saturation ($S_w = 0$) (i.e., 100% oil saturation). Strong capillary forces could affect the leakoff process at high oil saturations (accelerate or slow down, depending on the balance between capillary and viscous forces), becoming lower and less controlling of the process at low oil saturations. Previous work (Brattekås et al. 2014) showed that capillary forces in chalk at strongly water-wet conditions could dehydrate polymer gel and reduce its volume by up to 99%. Another previous study by the authors and others

(Brattekås et al. 2013) also indicated an influence of oil-wet conditions on gel dehydration; using computed-tomography imaging, we observed that the water saturation in the matrix of an oil-wet limestone did not change during gel injection (i.e., leakoff water did not enter the matrix when gel was injected at a low injection rate). Increasing the gel injection rate, and thus the differential pressure across the fracture, allowed leakoff close to the inlet end of the core, verified by an increasing water-saturation at the inlet end of the matrix. The pressure drop was not sufficient to allow water to travel the length of the matrix, and the water re-entered the gel-filled fracture to be produced through the fracture outlet. Hence volumetric measurements of effluents in core-scale experiments might not correctly reflect fluid flow within the system, and separate measurements of fracture and matrix flow do not ensure continuous transportation of the measured fluid through either. The use of small, strongly wetted core plugs in the present study also influenced the saturation development within each core half (see section on Gel Injection into Fractured, Oil-Saturated Core Plugs).

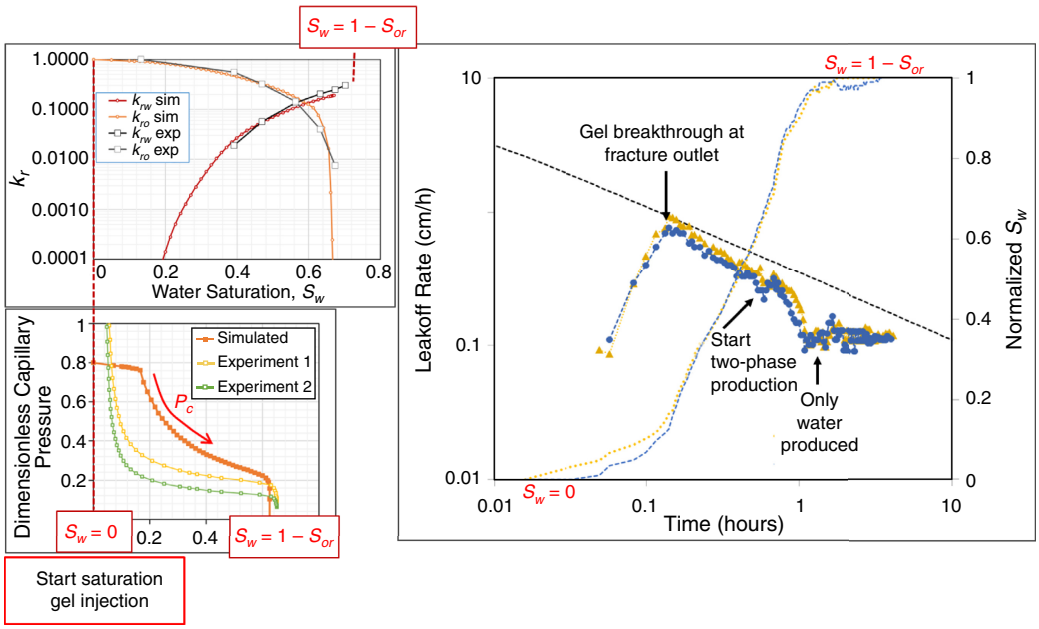

Fig. 13—The volumetrically measured leakoff rate deviated from the Seright model in oil-saturated limestone and chalk cores (this figure shows chalk cores). The leakoff behavior was consistent—high initial leakoff, but swiftly reduced during two-phase production. At the end of two-phase production, water alone was produced from the matrix, and the leakoff rate was close to constant. The relative permeability and capillary pressure curves shown on the left are representative of the chalk core material. The saturation at the start of gel injection was $S_w = 0$. The k_r and capillary pressure figures were modified from Andersen et al. (2018). k_r = relative permeability.

At S_{or}, capillary forces no longer aid (or limit) leakoff; the flow of water through the matrix is then controlled by the endpoint relative permeability to water $k_{rw,or}$ (flow within the rock matrix) and the gel (inflow of water to the matrix from gel). Leakoff in chalk, and its deviation from the conventional leakoff model, is shown in Fig. 13. A significant deviation between the expected and measured leakoff was observed at S_{or}, which cannot be related to the core shape or a capillary driven displacement front. Although flow within the matrix is limited by k_{rw}, this might not be the only explanation for the deviation: Strong capillary forces in the matrix [previously observed to reduce the gel volume by up to 99% without applying additional pressure on the gel (Brattekås et al. 2014)] could influence filter-cake formation in the adjacent fracture during gel injection, possibly drawing the gel closer and more evenly to the fracture surface and increasing the contribution to leakoff from the dehydrated gel layer. Both these effects limit the number of leakoff sites during late-stage gel injection, which can reduce the leakoff rate.

The experimental setup setup may also influence leakoff, specifically the use of 1/8-in. tubing drilled into the cores at the core circumference to represent the production outlet for both oil and water. The outlet was small relative to the leakoff area (fracture surface), and inflow of two fluid phases into the small area around the production tubing could cause a "choke effect," in which each fluid limits the flow of the other. This hypothesis was tested in chalk by implementing different production outlet designs, but no evidence of a choke effect was observed. Therefore, the original 1/8-in. outlets were used in the sandstone cores. In the current work, MRI showed that leakoff in chalk was controlled by the formation of a displacement front and less so by outlet properties. This, however, was not true for sandstone, where the magnitude and direction of the viscous pressure drop (implemented by gel) control the majority of matrix flow. An influence of outlet properties might explain the lower-than-expected leakoff rates in oil-saturated sandstone. Influences from outlet properties (e.g., from using 1/8-in. tubing as matrix production outlets) are more likely to occur in cores where the displacement front is nonexistent or less influential on fluid flow.

Deviations from conventional and expected leakoff behavior observed when the rock matrix is saturated by two phases instead of one can be attributed to saturation functions (e.g., a high capillary pressure causing the formation of a stable displacement front), properties of the gel (e.g., limited leakoff sites), and/or properties of the experiment (e.g., cylindrical core shape, outlet properties). Analyzing leakoff when gel dehydration is not solely dictated by gel or fracture properties must be done while considering possible influences from the matrix, the gel, and the experiment. Gel dehydration is influenced by both the gel/fracture properties and the matrix when capillary forces balance or overcome the viscous forces applied by gel (i.e., using two-phase-saturated rocks of strong wetting preference). This work indicated that the leakoff rate depends on whether or not a displacement front forms in the matrix, in addition to a demonstrated effect of core shape. The discussion included several factors that render core-scale experiments and reliable subsequent analysis challenging, especially in conventional experiments without imaging. A good example is the swift drop in leakoff observed during gel injection in oil-saturated chalk. This behavior is not a general characteristic of leakoff in oil-saturated chalk, nor can it be expected in all experiments; it is simply attributed to the presence of a stable displacement front moving through a nonuniformly shaped medium.

Using this or similar experimental results to represent leakoff on larger scales (e.g., during gel injection in a chalk reservoir) would not be advisable.

Upscaling to Field Applications. Reservoir rock is frequently saturated by more than one fluid, and fluid transport in fractured reservoirs, especially in low-permeability rock formations, relies on capillary forces. The shape of matrix blocks is not always uniform, and the wettability of the rock formation might have changed during ages of crude oil exposure. Hence, reservoirs that could be suitable candidates for polymer gel treatments can exhibit several of the factors identified in this work to influence leakoff. The conventional Carter and Seright leakoff models are based on water-saturated, high-permeability rock, where the leakoff behavior is most likely controlled by the properties of the gel and fracture network. In the near-well region, because of high viscous pressure gradients, leakoff may be determined by gel and the conventional models are correct. Basing entire reservoir predictions on these models, however, could fail to capture the true properties of many in-depth polymer gel treatments. The challenge is further complicated by the pitfalls of core-scale analysis identified in this work, where laboratory experiments without imaging could easily be misinterpreted. Good and representative modeling of gel behavior, and validation of controlled core-scale experiments with both imaging and modeling, is a possibility to overcome these challenges and improve predictions. Initial modeling of gel behavior during spontaneous imbibition is presented in Andersen et al. (2018).

Conclusions

- The leakoff rate must be clearly defined. For most applications, the volume of water leaving the gel is most important; this controls the rate of gel propagation into a reservoir and fracture growth during hydraulic fracturing. The representation of this leakoff rate as a 2D parameter is useful to account for variations in fracture volume between experiments.
- The leakoff rate can only be related to a velocity when leakoff water forms a stable displacement front parallel to, and moving away from, the fracture surface. The formation of such a front can be validated by imaging and relies, for example, on saturation functions (relative permeability and capillary pressure) and properties of the fluids, porous medium, and experimental setup.
- MRI was successfully used to track the leakoff front position during gel injection into oil-saturated chalk and identified the existence of a stable and capillary-driven displacement front in the rock matrix.
- In-situ imaging by MRI verified the swift decline in leakoff rate observed in oil-saturated chalk cores and explained the nonuniform shape of the rock matrix through which the leakoff displacement front moves. The volume ahead of the front quickly diminishes, which leads to a decrease in oil production. This behavior must not be mistaken for a general characteristic of leakoff in oil-saturated chalk.
- Saturation functions in the rock matrix can influence leakoff. We propose that leakoff deviates from conventional behavior when capillary forces in the matrix balance the viscous force applied on the system by gel. Positive capillary forces might support the formation of a stable displacement front in the matrix. Negative capillary forces (oil-wet preferences) might prevent leakoff water from entering the matrix. The leakoff rate will then no longer be controlled by gel only.
- Gel dehydration on the core scale must be analyzed while considering influences from the matrix (e.g., saturation functions, wettability), the gel (e.g., filter-cake formation, leakoff sites), and experimental properties (e.g., core shape, outlet properties).
- The rock matrix of a productive oil reservoir is often saturated by (at least) two phases. These factors can influence leakoff during gel injection into real reservoirs. Representative numerical modeling of the gel and gel/rock matrix interactions might provide improved core- and reservoir-scale predictions.

Nomenclature

H = height of fracture, cm
k = absolute permeability, md
k_r = relative permeability, dimensionless
k_{rw} = relative permeability of water, dimensionless
K_{ratio} = approximate permeability contrast between the core halves of a fractured system, dimensionless
L = length of core half or fracture, cm
$r_{\max}$ = maximum thickness of a core half (minimum distance between fracture and matrix production outlet), cm
S_o = oil saturation, dimensionless
S_{or} = residual oil saturation, dimensionless
S_w = water saturation, dimensionless
ϕ = porosity, dimensionless

Subscript

i = oil (o) or water (w)

Acknowledgments

In-situ imaging by MRI was performed at the Equinor MRI Research Centre at Sandsli, Bergen. The authors acknowledge Per Fotland for his valuable help during experiments. The authors acknowledge the Research Council of Norway and the industry partners, ConocoPhillips Skandinavia A/S, Aker BP ASA, Eni Norge A/S, Maersk Oil Norway A/S, Dong Energy A/S, Denmark, Statoil Petroleum A/S, Engie E&P Norge A/S, Lundin Norway A/S, Halliburton A/S, Schlumberger Norge A/S, and Wintershall Norge A/S of the National IOR Centre of Norway for support.

References

Andersen, P. Ø., Lohne, A., Stavland, A. et al. 2018. Core Scale Simulation of Spontaneous Solvent Imbibition From HPAM Gel. Presented at the SPE Improved Oil Recovery Conference, Tulsa, 14–18 April. SPE-190189-MS. https://doi.org/10.2118/190189-MS.

Barati, R., Hutchins, R., Friedel, T. et al. 2009. Fracture Impact of Yield Stress and Fracture-Face Damage on Production With a Three-Phase 2D Model. *SPE Prod & Oper* **24** (2): 336–345. SPE-111457-PA. https://doi.org/10.2118/111457-PA.

Brattekås, B. and Fernø, M. A. 2016. New Insight From Visualization of Mobility Control for Enhanced Oil Recovery Using Polymer Gels and Foams. In *Chemical Enhanced Oil Recovery (cEOR)—A Practical Overview*, ed. L. Romero-Zêron, Chap. 3, 101–121. London, UK: InTechOpen. https://doi.org/10.5772/61394.

Brattekås, B., Graue, A., and Seright, R. S. 2016. Low-Salinity Chase Waterfloods Improve Performance of Cr(III)-Acetate Hydrolyzed Polyacrylamide Gel in Fractured Cores. *SPE Res Eval & Eng* **19** (02): 331–339. SPE-173749-PA. https://doi.org/10.2118/173749-PA.

Brattekås, B., Haugen, Å., Ersland, G. et al. 2013. Fracture Mobility Control by Polymer Gel—Integrated EOR in Fractured, Oil-Wet Carbonate Rocks. Presented at the EAGE Annual Conference & Exhibition Incorporating SPE Europec, London, 10–13 June. SPE-164906-MS. https://doi.org/10.2118/164906-MS.

Brattekås, B., Haugen, Å., Graue, A. et al. 2014. Gel Dehydration by Spontaneous Imbibition of Brine From Aged Polymer Gel. *SPE J.* **19** (1): 122–134. SPE-153118-PA. https://doi.org/10.2118/153118-PA.

Brattekås, B., Pedersen, S. G., Nistov, H. T. et al. 2015. Washout of Cr(III)-Acetate-HPAM Gels From Fractures: Effect of Gel State During Placement. *SPE Prod & Oper* **30** (2): 99–109. SPE-169064-PA. https://doi.org/10.2118/169064-PA.

Dantas, T. N. C., Santanna, V. C., Dantas Neto, A. A. et al. 2005. Hydraulic Gel Fracturing. *J Disp Sci Techn.* **26** (1): 1–4. http://doi.org/10.1081/DIS-200040161.

Ekdale, A. A. and Bromley, R. G. 1993. Trace Fossils and Ichnofabric in the Kjølby Gaard Marl, Uppermost Cretaceous, Denmark. *Bull Geol Soc Denmark* **31:** 107–119.

Haugen, Å., Fernø, M. A., and Graue, A. 2008. Numerical Simulation and Sensitivity Analysis of In Situ Fluid Flow in MRI Laboratory Waterfloods of Fractured Carbonate Rocks at Different Wettabilities. Presented at the SPE Annual Technical Conference and Exhibition, Denver, 21–24 September. SPE-116145-MS. https://doi.org/10.2118/116145-MS.

Hild, G. P. and Wackowski, R. K. 1999. Reservoir Polymer Gel Treatments To Improve Miscible CO_2 Flood. *SPE Res Eval & Eng* **2** (2): 196–204. SPE-56008-PA. https://doi.org/10.2118/56008-PA.

Hjuler, M. L. and Fabricius, I. L. 2007. *Diagenesis of Upper Cretaceous Onshore and Offshore Chalk from the North Sea Area*. PhD thesis, Kgs. Lyngby: DTU Environment, Denmark (August 2007).

Howard, G. C. and Fast, C. R. 1957. Optimum Fluid Characteristics for Fracture Extension. *Drill & Prod Prac.* (1 January): 261–270. API-57-261.

Howard, G. C. and Fast, C. R. 1970. *Hydraulic Fracturing*. Richardson, Texas: Monograph Series, Society of Petroleum Engineers.

Johannesen, E. B. 2008. *NMR Characterization of Wettability and How it Impacts Oil Recovery in Chalk*. PhD thesis. Dept. of Physics and Technology, University of Bergen, Norway (May 2008).

Kantzas, A., Allsopp, K., and Marentette, D. 1999. Utilization of Polymer Gels, Polymer Enhanced Foams, and Foamed Gels for Improving Reservoir Conformance. *J Can Pet Technol* **38** (13): 1–8. PETSOC-99-13-58. https://doi.org/10.2118/99-13-58.

Klein, E. and Reuschle, T. 2003. A Model for the Mechanical Behaviour of Bentheim Sandstone in the Brittle Regime. In *Thermo-Hydro-Mechanical Coupling in Fractured Rock*, ed. H. J. Kümpel. Pageoph Topical Volumes, 833–849. Basel: Springer-Birkhäuser. https://doi.org/10.1007/978-3-0348-8083-1_3.

Liu, J. and Seright, R. S. 2001. Rheology of Gels Used for Conformance Control in Fractures. *SPE J.* **6** (02): 120–125. SPE-70810-PA. https://doi.org/10.2118/70810-PA.

Penny, G. S. and Conway, M. W. 1989. Fluid Leakoff. In *Recent Advances in Hydraulic Fracturing*, ed. H. L. Doherty, Vol. 12, 147–176. Richardson, Texas: Monograph Series, Society of Petroleum Engineers.

Portwood, J. T. 2005. The Kansas Arbuckle Formation: Performance Evaluation and Lessons Learned From More Than 200 Polymer-Gel Water-Shutoff Treatments. Presented at the SPE Production and Operations Symposium, Oklahoma City, Oklahoma, 16–19 April. SPE-94096-MS. https://doi.org/10.2118/94096-MS.

Schutjens, P. M. T. M., Hausenblas, M., Dijkshoorn, M. et al. 1995. The Influence of Intergranular Microcracks on the Petrophysical Properties of Sandstone—Experiments To Quantify Effects of Core Damage. Presented at the International Symposium of the Society of Core Analysts, San Francisco, 12–14 September. SCA-9524.

Seright, R. S. 1995. Gel Placement in Fractured Systems. *SPE Prod & Fac* **10** (4): 241–248. SPE-27740-PA. https://doi.org/10.2118/27740-PA.

Seright, R. S. 1999. Polymer Gel Dehydration During Extrusion Through Fractures. *SPE Prod & Fac* **14** (2): 110–116. SPE-56126-PA. https://doi.org/10.2118/56126-PA.

Seright, R. S. 2001. Gel Propagation Through Fractures. *SPE Prod & Fac* **16** (4): 225–231. SPE-74602-PA. https://doi.org/10.2118/74602-PA.

Seright, R. S. 2003a. An Alternative View of Filter-Cake Formation in Fractures Inspired by Cr(III)-Acetate-HPAM Gel Extrusion. *SPE Prod & Fac* **18** (1): 65–72. SPE-81829-PA. https://doi.org/10.2118/81829-PA.

Seright, R. S. 2003b. Washout of Cr(III)-Acetate-HPAM Gels From Fractures. Presented at the SPE International Symposium on Oilfield Chemistry, Houston, 5–7 February. SPE-80200-MS. https://doi.org/10.2118/80200-MS.

Seright, R. S., Lane, R. H., and Sydansk, R. D. 2003. A Strategy for Attacking Excess Water Production. *SPE Prod & Fac* **18** (3): 158–169. SPE-84966-PA. https://doi.org/10.2118/84966-PA.

Sydansk, R. D. and Southwell, G. P. 2000. More Than 12 Years Experience With a Successful Conformance-Control Polymer-Gel Technology. *SPE Prod & Oper* **15** (4): 270–278. SPE-66558-PA. https://doi.org/10.2118/66558-PA.

Tie, H. 2006. *Oil Recovery by Spontaneous Imbibition and Viscous Displacement From Mixed-Wet Carbonates*. PhD thesis, University of Wyoming, Laramie, Wyoming, USA.

Willhite, G. P. and Pancake, R. E. 2008. Controlling Water Production Using Gelled Polymer Systems. *SPE Res Eval & Eng* **11** (3): 454–465. SPE-89464-PA. https://doi.org/10.2118/89464-PA.

Bergit Brattekås is a reservoir physics researcher in the Department of Physics and Technology, University of Bergen, Norway. She was previously a post-doctoral degree researcher and project leader at the National IOR Centre of Norway. Brattekås' research interests are flow mechanisms in porous media and fractures, with an emphasis on the use of polymer gels or foam for increased sweep efficiency during carbon dioxide (CO_2) storage and EOR operations. She holds a PhD degree in reservoir physics from the University of Bergen.

Randy Seright has been a senior engineer at the New Mexico Petroleum Recovery Research Center at New Mexico Tech for the past 31 years. He holds a PhD degree in chemical engineering from the University of Wisconsin, Madison. Seright's work primarily involves using polymer and gels to improve sweep efficiency in reservoirs. He received the SPE/DOE IOR Pioneer Award in 2008.

Geir Ersland is an associate professor in reservoir physics at the Department of Physics and Technology at the University of Bergen. His scientific work is focused on flow in porous media, CO_2 storage in aquifers, CO_2 EOR, and gas hydrate in sediments.